

PAPER • OPEN ACCESS

## Magnetic and nonmagnetic impurity effects on $\text{Cu}_3\text{Mo}_2\text{O}_9$

To cite this article: Y Ebukuro *et al* 2018 *J. Phys.: Conf. Ser.* **969** 012110

View the [article online](#) for updates and enhancements.

You may also like

- [Study of the modified magnetic, dielectric, ferroelectric and optical properties in Ni substituted  \$\text{GdFe}\_{1-x}\text{Ni}\_x\text{O}\_3\$  orthoferrites](#)  
R S Arun Raj, S Meenu, Aruna Joseph et al.
- [Role of Ni substitution on structural, magnetic and electronic properties of epitaxial  \$\text{CoCr}\_2\text{O}\_4\$  spinel thin films](#)  
P Mohanty, S Chowdhury, R J Choudhary et al.
- [Effects of Ni Substitution on Structural, Dielectrical, and Ferroelectric Properties of Chemical-Solution-Deposited Multiferroic  \$\text{BiFeO}\_3\$  Films](#)  
S. K. Singh, R. Palai, K. Maruyama et al.



**ECS**  
The  
Electrochemical  
Society  
Advancing solid state &  
electrochemical science & technology

**DISCOVER**  
how sustainability  
intersects with  
electrochemistry & solid  
state science research

# Magnetic and nonmagnetic impurity effects on $\text{Cu}_3\text{Mo}_2\text{O}_9$

Y Ebukuro<sup>1</sup>, M Noda<sup>1</sup>, H Kuwahara<sup>1</sup>, H Kuroe<sup>1</sup>, M Hase<sup>2</sup>, K Oka<sup>3</sup>, T Ito<sup>3</sup> and H Eisaki<sup>3</sup>

<sup>1</sup> Sophia University, Chiyoda-ku, Tokyo 102-8554, Japan

<sup>2</sup> National Institute for Materials Science (NIMS), Tsukuba, Ibaraki 305-0047, Japan

<sup>3</sup> National Institute of Advanced Industrial Science and Technology (AIST), Tsukuba, Ibaraki 305-8562, Japan

E-mail: y-ebukuro0116@eagle.sophia.ac.jp

**Abstract.** We compare the magnetic (Ni) substitution effects in  $\text{Cu}_3\text{Mo}_2\text{O}_9$  to the nonmagnetic (Zn) ones. Changes in the lattice constants show similar behaviours for both impurity substituted samples. In specific heat measurements, we observe the anomalous specific heat at the phase transition temperature  $T_N$ .  $T_N$  in the Ni substituted sample increases to 8.8 K; while  $T_N$  in the Zn substituted sample decreases to 4.0 K. In magnetization measurement on the Ni substituted sample, we obtain the Van-Vleck type constant magnetization. We suggest the existence of the single-ion anisotropy of the substituted  $\text{Ni}^{2+}$  ions, which is a possible candidate for the origin of the increment of  $T_N$  in the Ni substituted sample.

## 1. Introduction

Impurity substitution effects have been extensively studied in the research field of magnetism. Controlling of magnetic properties by impurity substitution is an interesting issue not only in the viewpoint of science but also in the viewpoint of application. Sometimes impurity substitution induces a different long-range order from that in the parent material. This phenomenon has been studied in detail from the viewpoint of a new ordered state induced by disturbing the original ordered state in the parent material, i.e., "the order-by-disorder effect". As an example, we summarized the impurity substitution effect in an inorganic spin-Peierls material  $\text{CuGeO}_3$  [1-3]. It has been reported that spin-Peierls transition is suppressed by nonmagnetic  $\text{Zn}^{2+}$  ions substituted for  $\text{Cu}^{2+}$  ions in this material; instead, another antiferromagnetic phase with the easy axis parallel to the  $c$ -axis appears at low temperatures.

Comparison between the magnetic and the nonmagnetic impurity effects is also interesting. In  $\text{CuGeO}_3$ , the effects of the magnetic impurity substitution have been reported [4-6]. In the spin-Peierls phase where  $\text{Cu}^{2+}$  ions form nonmagnetic spin dimers,  $S = 0$   $\text{Zn}^{2+}$  and  $S = 1$   $\text{Ni}^{2+}$  ions introduce similar effects. i.e. the breaking of spin-singlet dimers. One difference occurs due to the single-ion anisotropy of  $S = 1$   $\text{Ni}^{2+}$  ions: the change of the easy axis almost parallel to the  $a$ -axis in the low temperature antiferromagnetic phase in Ni substituted sample.



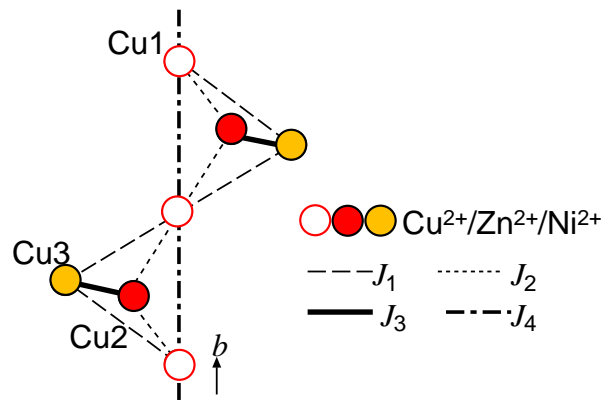


Figure 1: (color online) The schematics of the Cu sites forming the distorted tetrahedral spin chain of  $\text{Cu}_3\text{Mo}_2\text{O}_9$ . The colors of the circles and the numbers just after the symbols of chemical elements distinguish the crystallographically different sites from one another. The  $\text{Cu}^{2+}$  ions are magnetically interacted through the  $J_1$ - $J_4$  super-exchange paths distinguished by different line types.

In this paper, we discuss the similarity and the difference between magnetic and nonmagnetic impurity substitution effects on  $\text{Cu}_3\text{Mo}_2\text{O}_9$ . Figure. 1 shows a distorted tetrahedral quasi-one-dimensional spin structure made from  $\text{Cu}^{2+}$  ions in  $\text{Cu}_3\text{Mo}_2\text{O}_9$ . By substituting impurity ions ( $\text{Ni}^{2+}$  and  $\text{Zn}^{2+}$ ) for the  $\text{Cu}^{2+}$  ions, it is possible to change the path of the super-exchange interaction directly and to affect the frustration effect of  $\text{Cu}_3\text{Mo}_2\text{O}_9$  [7]. Because of the difference between the crystal radius of impurity ion and that of  $\text{Cu}^{2+}$  one [8], we need to consider the chemical pressure effect.

## 2. Experiments

As a starting material, we synthesized polycrystalline powder of  $(\text{Cu,Zn,Ni})_3\text{Mo}_2\text{O}_9$  with various impurity concentrations from a stoichiometric mixture of raw materials,  $\text{CuO}$ ,  $\text{NiO}$ ,  $\text{ZnO}$  and  $\text{MoO}_3$  by using a conventional solid-states reaction. We confirmed that the polycrystalline powder is single phase from the x-ray powder diffraction patterns. We obtain the lattice constants based on the orthorhombic crystal structure with the  $Pnma$  symmetry of the lattice. Recent result clearly shows that the monoclinic crystal structure with the  $P2_1/m$  symmetry of the lattice is more suitable at room temperature [9]. Because of the limited accumulation time, we did not observe the peak in the diffraction pattern identifying the  $P2_1/m$  lattice symmetry. The systematic change of the lattice constants at room temperature will be discussed later.

We prepared single crystals of  $\text{Cu}_3\text{Mo}_2\text{O}_9$ ,  $(\text{Cu,Zn})_3\text{Mo}_2\text{O}_9$  and  $(\text{Cu,Ni})_3\text{Mo}_2\text{O}_9$  with 5.0% of Ni or Zn concentration. The single crystal of each sample was synthesized from the pressed powder with a rod shape by using the continuous solid-state crystallization method, which is based on the solid state reaction [10]. We assume that the impurity concentration in the single crystal is the same as that in the starting polycrystalline powder because the powder is not melt in this process. We determined the crystal axes by using Laue photograph and cut them into a rectangular parallelepiped of which surface vectors toward each crystal axis.

The temperature dependence of specific heat at 0 T was measured by using Quantum Design Physical Properties Measurement System (PPMS). The temperature dependences of magnetization under static magnetic field of 0.1 T were measured by using Quantum Design Magnetic Properties Measurement System (MPMS-XL).

### 3. Results

#### 3.1 Lattice constants at room temperature

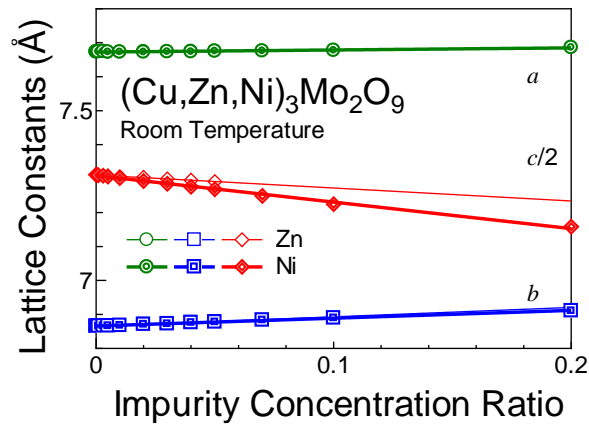


Figure 2: (color online) Lattice constants as functions of impurity concentration ratio.

**Table 1:** Spin moments, crystal radii referred from ref. [8] and the mass numbers of some ions. The crystal radii are determined by considering the number of oxygen ions around each ion, i.e., five (six) oxygen ions surround the Cu1 site (the Cu2 and Cu3 sites).

Ions	$S$	Crystal Radius for Cu1 site (Å)	Crystal Radius for Cu2 and Cu3 sites (Å)	Mass Number
$\text{Ni}^{2+}$	1	0.83	0.77	58.69
$\text{Cu}^{2+}$	1/2	0.87	0.79	63.55
$\text{Zn}^{2+}$	0	0.88	0.82	65.39

Figure 2 compares the lattice constants in Ni and Zn substituted samples as functions of impurity substitution ratio. The qualitative trends of the changes of the lattice constants in the Ni and the Zn substituted samples are similar with each other. The change of lattice constant along the  $c$ -axis in the Ni substituted samples is larger than that in the Zn substituted ones. The lattice constants along the  $a$ - and the  $b$ -axes have similar trends in both substituted samples. According to Table I, the crystal radius of  $\text{Zn}^{2+}$  ion is larger than that of  $\text{Cu}^{2+}$  ions but  $\text{Ni}^{2+}$  one is smaller. It seems that this result was not expected from a standard chemical pressure model based on the packing of the rigid spheres with the average crystal radii. This is the unexpected similarity between magnetic and nonmagnetic impurity substitution effects.

### 3.2 Specific heat

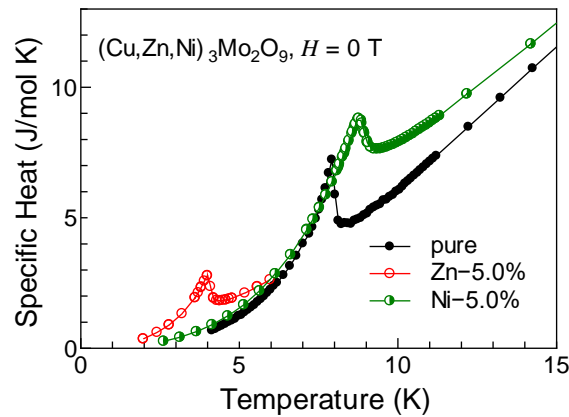


Figure 3: (color online) Temperature dependences of specific heats in  $\text{Cu}_3\text{Mo}_2\text{O}_9$  and the Zn-5.0% and the Ni-5.0% substituted samples.

Figure 3 shows the temperature dependences of the specific heats (the  $C$ - $T$  curves) in  $(\text{Cu,Zn,Ni})_3\text{Mo}_2\text{O}_9$ . We observed an anomalous specific heat, the jump of  $C$  due to the second-order phase transition, in each  $C$ - $T$  curve. The peaks in the impurity substituted samples are rounded. We define  $T_N$  as the temperature which gives the local maximum of the  $C$ - $T$  curve. We estimated  $T_N$  in the Zn-5.0% and the Ni-5.0% substituted samples as 4.0 and 8.8 K, respectively, which are lower and higher than  $T_N$  in the parent material. This is the unexpected difference between magnetic and nonmagnetic impurity substitution effects.

### 3.3 Magnetization

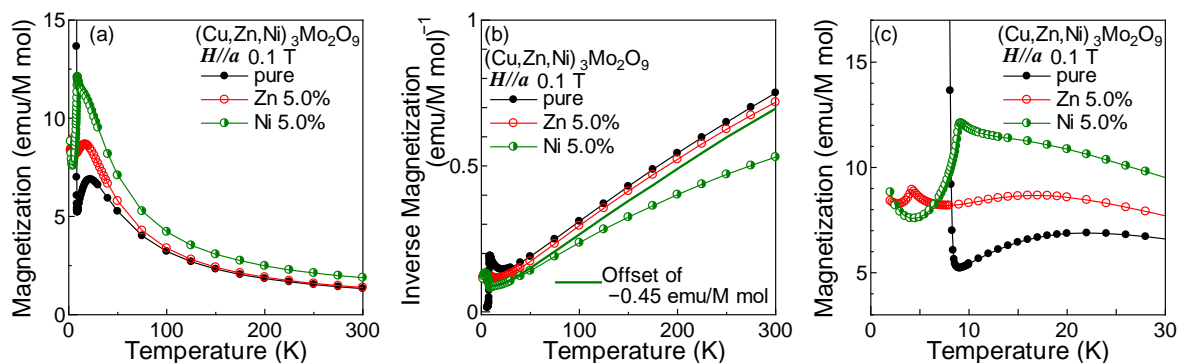


Figure 4: (color online) (a) Temperature dependences of magnetization at 0.1 T along the  $a$ -axis in  $\text{Cu}_3\text{Mo}_2\text{O}_9$  and the Zn-5.0% and the Ni-5.0% substituted samples. (b) Inverse magnetization of (a). (c) Low temperature expansion of (a).  $M$  in the unit of the ordinate denotes magnetic ions ( $\text{Cu}^{2+}$  and  $\text{Ni}^{2+}$ ).

Figure 4(a) shows the temperature dependences of magnetization  $M_a$  along the  $a$ -axis in  $(\text{Cu,Zn,Ni})_3\text{Mo}_2\text{O}_9$ . In this work, we show  $M_a$  for one mole of the magnetic ions. One can see in all panels in Fig. 4 that the Ni substitution increases  $M_a$ . The high temperature magnetization seems to be Curie-Weiss type. To estimate the gain and the offset parameters, we show  $M_a^{-1}$  as functions of temperature in Fig. 4(b). One can see that the temperature dependence of  $M_a^{-1}$  in the Ni substituted sample is very different from other two temperature dependences. When we subtract 0.45 emu/M mol from  $M_a$  in the Ni substituted sample, as shown with the bold curve in Fig. 4(b),  $(M_a - 0.45)^{-1}$  has a similar slope with  $M_a^{-1}$  of  $\text{Cu}_3\text{Mo}_2\text{O}_9$  and the Zn substituted sample in the wide temperature range. The small difference between  $(M_a - 0.45)^{-1}$  in the Ni substituted sample and  $M_a^{-1}$  in other two samples might

be explained with the change of Weiss temperature. The origin of offset is Van-Vleck type temperature independent magnetization which is possible even in the isolated  $S = 1$   $\text{Ni}^{2+}$  ions.

As shown in Fig. 4(c), the strong enhancement of  $M_a$  below  $T_N$  is observed in the parent material [7]. This is due to the order of weak ferromagnetic component of the spin moments under magnetic fields, which reflects the temperature dependence of the order parameter [11]. Instead of this increment, we observed the reduction of  $M_a$  with decreasing temperature in the Zn and the Ni substituted samples. In our previous report [11], we explained this reduction in the Zn-5.0% substituted sample as cusp-shaped temperature dependence. In the Ni-5.0% substituted sample, we observed similar temperature dependence with very different  $T_N$ , i.e.,  $M_a$  rapidly decreases with decreasing temperatures just below  $T_N$ . We defined  $T_N$  as the temperature at which  $\partial M/\partial T$  had local maximum.  $T_N$  in the Zn and the Ni substituted samples are 4.2 and 9.0 K, respectively. The values are slightly ( $\sim 0.2$  K) higher than  $T_N$  estimated based on the results of the specific heat. This trend is consistent with our previous report [12]. Once the  $M_a$  dropped just below  $T_N$ , a Curie-Weiss-type increment of  $M_a$  with decreasing temperature was observed at the lowest temperature region in our measurements. This term in the Ni substituted sample is larger than that of Zn substituted one.

Above  $T_N$ , we observed broad peaks of  $M_a$ , which reflects the quasi-one dimensionality of  $\text{Cu}_3\text{Mo}_2\text{O}_9$  [7]. In the impurity substituted samples, the temperature at which  $M_a$  show local maximum is slightly lower than that in the parent material. This suggests that the quasi-one dimensionality of the magnetic system is suppressed or the amplitude of the effective magnetic interaction is lowered by impurity substitutions.

#### 4. Discussion

Let us discuss the origin of the increment of  $T_N$  upon the Ni substitution. When the easy axis or the easy plane induced by the single-ion anisotropy of  $\text{Ni}^{2+}$  ions is consistent with (or not conflict with) the magnetic anisotropy in the antiferromagnetic phase of the parent material, Ni substitution has the potential to stabilize the magnetic order and to increase  $T_N$ . However, breaking of translational symmetry due to impurity substitution suppresses long-range order of the spin system, which decrease  $T_N$ . Due to the competitive balance of the above two effects, there is a possibility that the Ni and the Zn substituted samples show the different substitution-ratio dependences with each other. The difference of  $T_N$  between the Ni and the Zn substituted  $\text{La}_2\text{CuO}_4$  is a good example [13-15].  $\text{La}_2\text{CuO}_4$ , which is known as the parent material of the high-temperature superconductor, has an antiferromagnetic  $\text{CuO}_2$  plane and has the antiferromagnetic phase at which the  $S = 1/2$  spins lying in the  $\text{CuO}_2$  plane [16].  $\text{La}_2\text{NiO}_4$  has the similar crystal structure and has the antiferromagnetic phase at which the  $S = 1$  spins lying in the  $\text{NiO}_2$  plane [17]. Because of the single-ion anisotropy of the  $\text{Ni}^{2+}$  ions, the spin direction in the antiferromagnetic phase is different from that in  $\text{La}_2\text{CuO}_4$  [15]. When the  $\text{Ni}^{2+}$  ions are introduced as a magnetic impurity into  $\text{La}_2\text{CuO}_4$ , they do not break the magnetic anisotropy in the  $\text{CuO}_2$  plane of the parent material. Moreover,  $\text{Ni}^{2+}$  ions interact antiferromagnetically with the surrounding  $\text{Cu}^{2+}$  ions, which hardly breaks the antiferromagnetic long-range order. Even in the Ni-30% substituted sample,  $T_N$  is almost unchanged. Zn substitution as a nonmagnetic impurity doping breaks the antiferromagnetic long-range order composed of the  $\text{Cu}^{2+}$  ions, which decreases  $T_N$  [13-16, 18].

We discuss the single-ion anisotropy in  $\text{Cu}_3\text{Mo}_2\text{O}_9$ . We observed Van-Vleck temperature-independent paramagnetic term in  $M_a$  as shown in Figs. 4(a) - 4(c). According to the Pryce's Hamiltonian [19], single-ion anisotropy is also expected to appear in the Ni substituted sample because both of these come from the spin-orbit interaction. To discuss in more details, we should know the precise direction of the quantum axis of  $\text{Ni}^{2+}$  ions, which is beyond the scope of this paper. Below  $T_N$ , spins of substituted  $S = 1$   $\text{Ni}^{2+}$  ions point a fixed direction in the lattice, which generates an internal magnetic field. When this internal magnetic field encourages antiferromagnetic order, it makes  $T_N$  higher. We conclude that this is the origin of the increment of  $T_N$  upon the Ni substitution.

One may think that the systematic change of the crystal radius listed in Table 1 may cause a chemical pressure effect. Because the lattice constants in both of the Zn and the Ni substituted samples have the same impurity-concentration dependences as shown in Fig. 2. We consider it cannot be the origin of the

change in  $T_N$ .

The Curie-Weiss type increment of  $M_a$  at low temperatures is probably due to the almost free spin induced by the impurity substitution, which might be related to the magnetic structure of the parent material. According to the recent result of powder neutron diffraction [9], the spins at the Cu1 site is almost nonmagnetic. The magnitude of spin moments at the Cu2 and Cu3 sites are  $(0.50 \sim 0.74)\mu_B$ , where  $\mu_B$  denotes the Bohr magneton. This strongly suggests that the magnetic ground state of this system includes the component of spin singlet state. In spin-Peierls system  $\text{CuGeO}_3$  [1-3], as stated in the previous section, nonmagnetic impurities suppress the formation of spin singlet state and introduce spin moments. In case of the Ni substitution [4-6], the spin moment of  $\text{Ni}^{2+}$  ion also breaks the spin-singlet state. The similarity between magnetic and nonmagnetic impurity substitution effects, the appearance of the Curie-Weiss term in both of the Ni and the Zn substituted samples, suggests the existence of the component of the spin singlet state in the magnetic ground state of  $\text{Cu}_3\text{Mo}_2\text{O}_9$ .

## 5. Conclusion

We compared the magnetic (Ni) substitution effects in  $\text{Cu}_3\text{Mo}_2\text{O}_9$  to the nonmagnetic (Zn) ones. Changes in the lattice constant showed the similar behaviors qualitatively for both impurity substituted samples. In specific heat measurements, we estimated  $T_N$  in the Zn-5.0% and the Ni-5.0% substituted samples as 4.0 and 8.8 K, respectively. In magnetization measurements on the Ni substituted sample, we obtained the Van-Vleck type temperature independent magnetization. We clarified the existence of the single-ion anisotropy of the substituted  $\text{Ni}^{2+}$  ions, which is a possible candidate for the origin of the increment of  $T_N$  in the Ni substituted sample.

## References

- [1] Hase M *et al.* 1993 *Phys. Rev. Lett.* **70** 3651
- [2] Hase M *et al.* 1993 *Phys. Rev. Lett.* **71** 4059
- [3] Hase M *et al.* 1995 *Physica B* **215** 164
- [4] Koide N *et al.* 1998 arXiv:cond-mat/9805095 [cond-mat.str-el]
- [5] Koide N *et al.* 1996 *Czech J. Phys.* **46** 1981
- [6] Grenier B *et al.* 2002 *Phys. Rev. B* **65** 094425
- [7] Hamasaki T *et al.* 2008 *Phys. Rev. B* **77** 134419
- [8] Shannon R D 1976 *Acta. Cryst. A* **32** 751
- [9] Hase M *et al.* 2015 *Phys. Rev. B* **92** 054425
- [10] Oka K *et al.* 2011 *J. Cryst. Growth* **334** 108
- [11] Kuroe H *et al.* 2014 *JPS Conf. Proc.* **2** 010206
- [12] Hirata Y *et al.* 2015 *Phys. Procedia* **75** 134
- [13] Ting S T *et al.* 1992 *Phys. Rev. B* **18** 11772
- [14] Machi T *et al.* 2003 *Physica C* **233** 388
- [15] Hiraka H *et al.* 2005 *J. Phys. Soc. Jpn.* **74** 2197
- [16] Vaknin D *et al.* 1987 *Phys. Rev. Lett.* **58** 2802
- [17] Aeppli G *et al.* 1988 *Phys. Rev. Lett.* **61** 203
- [18] Uchinokura K *et al.* 1995 *Physica B* **205** 234
- [19] Pryce M H L 1950 *Proc. Phys. Soc. A* **63** 25